Thermodynamics of the oxidation of ZrB_2–TiB_2, ZrB_2–SiC and ZrB_2–B_4C ceramics

SHIRSHENDU CHAKRABORTY[1], PROBAL KUMAR DAS[1] and DINABANDHU GHOSH[2,*]

[1]CSIR-Central Glass and Ceramic Research Institute, Kolkata 700032, India
[2]Department of Metallurgical and Materials Engineering, Jadavpur University, Kolkata 700032, India
*Author for correspondence (dbghosh100@yahoo.com)

Abstract.   The thermodynamics of the oxidation of three-high temperature ZrB_2-based ceramics (ZrB_2–TiB_2, ZrB_2–SiC and ZrB_2–B_4C) has been studied in order to find the stability domain of zirconium diboride, in terms of temperature, partial pressure of oxygen and composition, in which it is protected against oxidation. In the case of the ZrB_2–TiB_2 binary system, a plot of log p_{O_2} *vs.* $1/T$ in the temperature range of 500–2000 K and another plot of p_{O_2} ($\times 10^{14}$) *vs.* x_{TiB_2} for $T = 2000$ K are made taking into account the two-extreme possibilities of no solubility and 100% solid solubility between ZrB_2 and TiB_2, respectively. A plot of log p_{CO} *vs.* log p_{O_2} is made for 1773 K for the systems ZrB_2–SiC and ZrB_2–B_4C. It was found that the ZrB_2–TiB_2 ceramics does not have sufficient oxidation resistance in the temperature range of 500–2000 K. ZrB_2 of ZrB_2–SiC ceramics can be protected under 1 atmosphere oxygen or in air if the liquid borosilicate (with the chosen composition, 70% B_2O_3–30% SiO_2), which is an intermediate product, provides a kinetic barrier to the continuation of oxidation by forming an impervious layer on the exposed surfaces. In contrast, the ZrB_2–B_4C ceramics does not produce the borosilicate upon oxidation. In view of the volatility of pure liquid B_2O_3, it is recommended that the ZrB_2–B_4C ceramics can be used at a lower temperature, perhaps below 1373 K, when the vapour pressure of B_2O_3 is significantly small.

Keywords.   Thermodynamics; stability diagram; oxidation; ZrB_2-based ceramics.
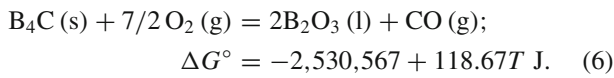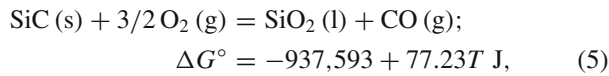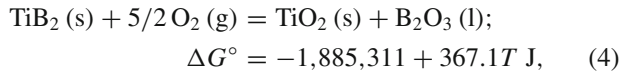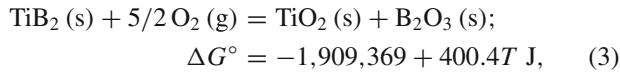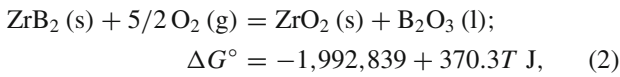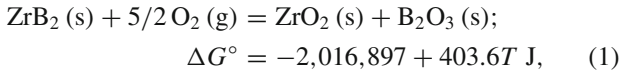
1. Introduction

Of all ultra-high temperature ceramics, zirconium diboride possesses unique combination of low density, high-melting temperature, high hardness and strength and good electrical and thermal conductivity [1–4]. These properties make it suitable for leading edges in aircraft and re-entry vehicles, as well as for high-temperature structural applications. Moreover, ZrB_2 does not undergo any phase transformation during high-temperature use, and its oxide also withstands high temperature. The oxidation resistance of ZrB_2, alone or in combination with SiC or other borides/carbides, has been reported by many investigators [5–11]. Notably, Peng and Speyer [10] studied the oxidation resistance of pore-free pressureless-sintered and post-hot isostatic pressed ZrB_2–B_4C (with varying concentrations of SiC) ceramics with the help of scanning thermogravimetry, over a range of temperatures. Specimens were heated in flowing air (flow rate of 0.1 l min^{-1}) from room temperature (298 K) at 50° min^{-1} to 1223 K, 30° min^{-1} to 1343 K, 10° min^{-1} to 1373 K, 5° min^{-1} to 1423 K and finally 3° min^{-1} to 1823 K. Crystalline phases in the oxidized samples were identified by X-ray diffraction and their microstructures were examined by scanning electron microscopy. Guo and Zhang [11] studied the oxidation behaviour of ZrB_2–SiC ceramics containing

10 and 30 vol% SiC in air at 1773 K for 0.5–10 h. The post-oxidation microstructural features were examined. The oxidation kinetics was analysed on the basis of weight gain, glass (borosilicate) layer thickness and the extended SiC-depleted layer thickness. The kinetics of oxidation has also been extensively studied in several other research groups [12–16]. Even so, a complete thermodynamic analysis of the oxidation of ZrB_2-based ceramics has not been available in the literature so far. Particularly, the construction of stability diagrams showing the stability domains of different phases as a function of temperature, oxygen pressure and composition (of the solid solution of two borides, say) has not been given due importance. These diagrams furnish the equilibrium products of oxidation as well as the condition under which no oxidation may occur. The objective of the present work is, accordingly, to draw such stability diagrams for each of three important ZrB_2-based systems, ZrB_2–TiB_2, ZrB_2–SiC and ZrB_2–B_4C, and to find the conditions under which ZrB_2 is protected in an oxygen environment.

2. Construction of the stability diagrams

The following data [17] for the standard free-energy changes as a function of temperature are used for the construction of

the stability diagrams for the systems ZrB_2–TiB_2, ZrB_2–SiC and ZrB_2–B_4C:

$$ZrB_2 \text{ (s)} + 5/2\,O_2 \text{ (g)} = ZrO_2 \text{ (s)} + B_2O_3 \text{ (s)};$$
$$\Delta G^\circ = -2{,}016{,}897 + 403.6T \text{ J,} \quad (1)$$

$$ZrB_2 \text{ (s)} + 5/2\,O_2 \text{ (g)} = ZrO_2 \text{ (s)} + B_2O_3 \text{ (l)};$$
$$\Delta G^\circ = -1{,}992{,}839 + 370.3T \text{ J,} \quad (2)$$

$$TiB_2 \text{ (s)} + 5/2\,O_2 \text{ (g)} = TiO_2 \text{ (s)} + B_2O_3 \text{ (s)};$$
$$\Delta G^\circ = -1{,}909{,}369 + 400.4T \text{ J,} \quad (3)$$

$$TiB_2 \text{ (s)} + 5/2\,O_2 \text{ (g)} = TiO_2 \text{ (s)} + B_2O_3 \text{ (l)};$$
$$\Delta G^\circ = -1{,}885{,}311 + 367.1T \text{ J,} \quad (4)$$

$$SiC \text{ (s)} + 3/2\,O_2 \text{ (g)} = SiO_2 \text{ (l)} + CO \text{ (g)};$$
$$\Delta G^\circ = -937{,}593 + 77.23T \text{ J,} \quad (5)$$

$$B_4C \text{ (s)} + 7/2\,O_2 \text{ (g)} = 2B_2O_3 \text{ (l)} + CO \text{ (g)};$$
$$\Delta G^\circ = -2{,}530{,}567 + 118.67T \text{ J.} \quad (6)$$

2.1 System ZrB_2–TiB_2

Two-extreme cases are considered regarding the solid solubility of ZrB_2 and TiB_2: (i) no solid solubility and (ii) 100% solid solubility. The data given in equations (1)–(4) are utilized to draw the stability diagrams.

2.1a No solid solubility: By using the thermodynamic relation $\Delta G^\circ = -RT \ln K$ (where R is the universal gas constant, $8.314 \text{ J K}^{-1} \text{ mol}^{-1}$; T, the temperature (Kelvin) and K, the equilibrium constant in terms of activities), equation (1) yields the relation:

$$-2{,}016{,}897 + 403.6T = 5/2\,RT \ln p_{O_2}. \quad (7)$$

It may be noted that $K = (a_{ZrO_2} \cdot a_{B_2O_3})/(a_{ZrB_2} \cdot (p_{O_2})^{5/2})$, in which the activities (a) of pure condensed phases such as ZrB_2 (s), ZrO_2 (s) and B_2O_3 (s) are unity and $a_{O_2} = p_{O_2}$. Equation (7) is used to plot log p_{O_2} *vs.* $1/T$ as line AB, which is extended over the temperature range of 500–723 K (melting point of B_2O_3) in figure 1. Above line AB, ZrO_2 (s) and B_2O_3 (s) are stable, and below it, ZrB_2 (s) is stable. In an exactly similar manner, line BC is drawn in the temperature range of 723–2000 K by plotting the following relation, obtained from equation (2):

$$-1{,}992{,}839 + 370.3T = 5/2\,RT \ln p_{O_2}. \quad (8)$$

Above line BC, ZrO_2 (s) and B_2O_3 (l) are stable, and below line BC, ZrB_2 (s) is stable.

The oxidation of TiB_2 is shown by lines EF (in the temperature range of 500–723 K) and FG (in the temperature range of 723–2000 K), which are drawn by using the following two relations, obtained from equations (3 and 4), respectively:

$$-1{,}909{,}369 + 400.4T = 5/2\,RT \ln p_{O_2}, \quad (9)$$
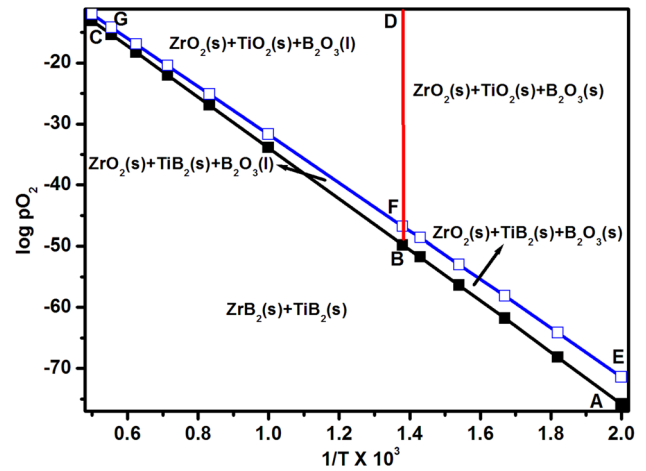
Figure 1. Stability diagram of the ZrB_2–TiB_2 system showing the stability fields of the boride and oxide mixtures in the temperature range of 500–2000 K, assuming no solid solubility of the two borides.
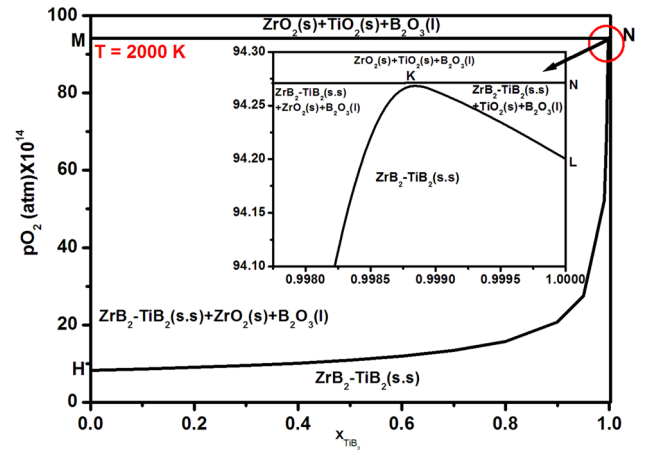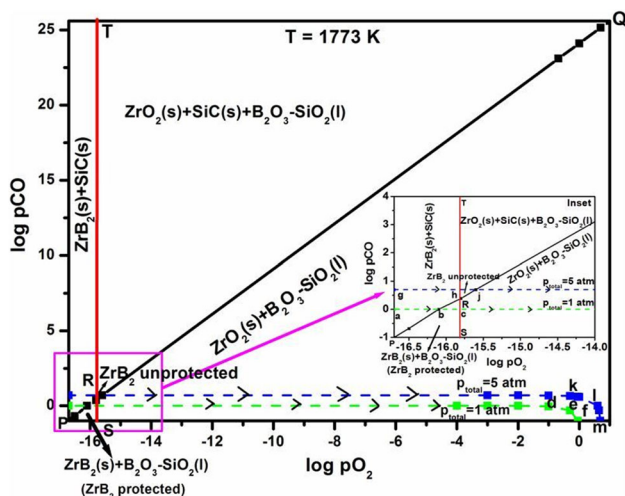

Figure 2. Stability diagram of the ZrB_2–TiB_2 system showing the stability fields of the boride and oxide mixtures at 2000 K, assuming complete solid solubility of the two borides.

$$-1{,}885{,}311 + 367.1T = 5/2\,RT \ln p_{O_2}. \quad (10)$$

Above lines EF and FG, TiO_2 and B_2O_3 (s/l) are stable, and below the line TiB_2 (s) is stable. The vertical line BD, drawn at 723 K (melting point of B_2O_3), separates B_2O_3 (s) from B_2O_3 (l).

2.1b 100% Solid solubility: Because the composition of the ZrB_2–TiB_2 solid solution is a variable in the present case, the stability diagram (figure 2) is constructed in a different way. A plot of p_{O_2} *vs.* x_{TiB_2} (x represents mole fraction) at 2000 K generates the curves HK and LK. The curve HK represents the equilibrium given by equation (2) and the curve LK represents the equilibrium given by equation (4). Assuming that ZrB_2 and TiB_2 form ideal solid solution ($a_i = x_i$),

Figure 3. Stability diagram of the ZrB_2–SiC system showing the stability fields of the oxide, boride and carbide mixtures at 1773 K, considering 70 mol% B_2O_3 in liquid borosilicate. The dotted isobaric curve *abcdef*, for $p_{total} = p_{O_2} + p_{CO} = 1$ atm, represents the thermodynamic progress of the oxidation, shown by arrows, of the ceramic ZrB_2–SiC under 1 atm O_2 at 1773 K; similarly, the dotted isobaric curve *ghjklm* for 5 atm O_2 at 1773 K.

equations (2 and 4), at 2000 K, yield the following two relations:

$$5.08 \times 10^{32} = 1/(x_{ZrB_2} \cdot p_{O_2}^{5/2}), \tag{11}$$

$$1.16 \times 10^{30} = 1/(x_{TiB_2} \cdot p_{O_2}^{5/2}). \tag{12}$$

Solving these two equations, with $x_{ZrB_2} = 1 - x_{TiB_2}$, the value of x_{TiB_2} is found to be 0.998 and p_{O_2} is 9.43×10^{-13} atm. These two values represent point K. Above line MKN, the boride mixture is fully converted into oxides. In the area enclosed by MK and HK, ZrB_2 is partially oxidized and in the area enclosed by NK and LK, which is negligibly small, TiB_2 is partially oxidized.

2.2 System ZrB_2–SiC

Because two of the oxidation products of this system, namely B_2O_3 and SiO_2, enter into a liquid phase (borosilicate) formation, the stability diagram (figure 3) is drawn, by plotting log p_{CO} vs. p_{O_2}, for $T = 1773$ K and for a particular liquid composition of 70 mol% B_2O_3–30 mol% SiO_2 in view of the reported [11] superior oxidation resistance of ZrB_2–30 vol% SiC (ZB30S). The equilibrium constant of equation (5) at 1773 K gives $K = 3.88 \times 10^{23} = (a_{SiO_2} \cdot p_{CO})/(a_{SiC} \cdot p_{O_2}^{3/2})$, which yields, after substituting $a_{SiO_2} = x_{SiO_2}$ (assuming ideal solution) $= 0.3$ and $a_{SiC} = 1$ (pure), the following equilibrium relation representing line PRQ:

$$\log p_{CO} = 3/2 \log p_{O_2} + 24.1. \tag{13}$$
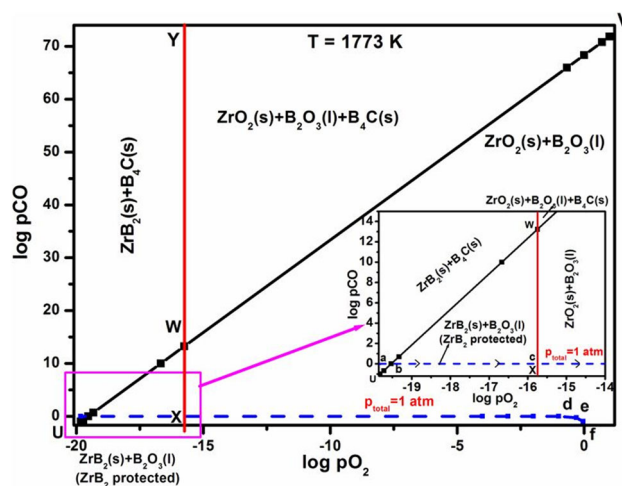
Figure 4. Stability diagram of the ZrB_2–B_4C system showing the stability fields of the oxide, boride and carbide mixtures at 1773 K. The dotted isobaric curve *abcdef*, for $p_{total} = p_{O_2} + p_{CO} = 1$ atm, represents the thermodynamic progress of the oxidation, shown by arrows, of the ceramic ZrB_2–B_4C under 1 atm O_2 at 1773 K.

Similarly, the equilibrium relation obtained from equation (2), after substituting $a_{B_2O_3} = x_{B_2O_3}$ (ideal solution) $= 0.7$, represents the vertical line SRT and is

$$\log p_{O_2} = -15.81. \tag{14}$$

Above line PRQ, SiC is stable and below it, impure SiO_2 (l) is stable. Similarly, on the left of line SRT, ZrB_2 is stable and on its right, ZrO_2 and impure B_2O_3 (l) are stable. Two-isobaric curves (*abcdef* and *ghjklm*) representing the total pressure ($p_{O_2} + p_{CO}$) of 1 and 5 atm, respectively, are superimposed on the stability diagram to show the course of oxidation of the ZrB_2–SiC mixture under 1 and 5 atm oxygen pressure.

2.3 System ZrB_2–B_4C

Because the oxidation products, in this case, include pure liquid B_2O_3, besides solid ZrO_2, the construction of the stability diagram (figure 4), drawn for 1773 K, is simpler. The equilibrium constant of equation (6) at 1773 K gives $K = 2.28 \times 10^{68} = ((a_{B_2O_3})^2 \cdot p_{CO})/(a_{B_4C} \cdot p_{O_2}^{7/2})$, which yields, after substituting each activity (*a*) as 1, the following equilibrium relation representing line UWV:

$$\log p_{CO} = 7/2 \log p_{O_2} + 68.36. \tag{15}$$

Similarly, the equilibrium relation obtained from equation (2) represents the vertical line XWY and is

$$\log p_{O_2} = -15.75. \tag{16}$$

Above line UWV, B_4C is stable and below it, B_2O_3 is stable. Similarly, on the left of line XWY, ZrB_2 is stable and on its right, ZrO_2 and B_2O_3 are stable. The isobaric curve (*abcdef*) representing the total pressure ($p_{O_2} + p_{CO}$) of 1 atm is superimposed on the stability diagram to show the course of oxidation of the ZrB_2–B_4C mixture under 1 atm oxygen pressure.

3. Discussion

3.1 *System ZrB_2–TiB_2*

3.1a *No solid solubility*: In figure 1, line BC presents a greater protective range for ZrB_2 than line AB in terms of partial pressure of oxygen, as a function of temperature ($T > 723$ K). Similarly, line FG presents a greater protective range for TiB_2 than line EF in terms of partial pressure of oxygen, as a function of temperature ($T > 723$ K). Below these two lines, ZrB_2 and TiB_2, respectively, are free from oxidation. However, these protective limits of oxygen pressure, say 10^{-13} atm at 2000 K for ZrB_2, are far too small, compared to the atmospheric oxygen. Accordingly, ZrB_2 will oxidize in air forming the two oxides ZrO_2 and B_2O_3. It is required to be seen that if the consideration of 100% solid solubility between the two borides will give any greater oxidation protection for the two borides, particularly ZrB_2.

3.1b *100% Solid solubility*: As the thermodynamic activity (and hence the mole fraction) of ZrB_2 in solid solution with TiB_2 progressively decreases from 1, along line HK in figure 2, the equilibrium partial pressure of oxygen for the oxidation of ZrB_2, according to equation (2), progressively increases and reaches the maximum value of about 10^{-12} atm at point K. The composition of the solid alloy corresponding to point K is 99.8 mol% TiB_2 and 0.2 mol% ZrB_2. Thus, the protective p_{O_2} limit for the oxidation of ZrB_2 increases at the most by about a factor of 10 when ZrB_2 is brought in solution with TiB_2. This value is much higher than the atmospheric oxygen and the oxidation of the borides is inevitable. It is to be noted that at a temperature <2000 K, the protection range of oxygen partial pressure is even lowered. If only the temperature of the system is >2000 K, which is uncommon, the equilibrium partial pressure for oxidation, and hence the protection range, will somewhat increase. So, it can be concluded that there is not much scope for the prevention of oxidation of ZrB_2–TiB_2 ceramics.

3.2 *System ZrB_2–SiC*

Zirconium diboride is protected, as shown in figure 3, in the domain PRS as well as in the domain enclosed by TRP (above line PR and on the left of line TR). According to the equilibrium diagram, the ZrB_2–SiC composite should be fully oxidized to ZrO_2 (s) and B_2O_3–SiO_2 (l) under 1 atm oxygen pressure. The thermodynamic path of oxidation of the

ZrB_2–SiC (s) mixture to ZrO_2 (s) and B_2O_3–SiO_2 (l) under 1 atm oxygen pressure can be tracked by moving from *a* to *f* along the line *abcdef* drawn for 1 atm total pressure ($p_{O_2} + p_{CO} = 1$) and superimposed on the stability diagram of figure 3. The relevance of this curve is that when the ZrB_2–SiC mixture is exposed to 1 atm O_2, the resulting gas composition will contain the product gas CO and the unreacted O_2 at the total pressure of 1 atm, satisfying the equilibrium constant of reaction (5). Therefore, an isobaric line for 1 atm ranging from 100% CO to 100% O_2 will cover all the possibilities of equilibrium gas composition when the ZrB_2–SiC composite is exposed to 1 atm oxygen. For example, point b represents the equilibrium of reaction (5), which is the first stage of oxidation, with equilibrium values $p_{CO} \approx 1$ atm and $p_{O_2} \approx 10^{-16}$ atm. Upon complete conversion of ZrB_2 + SiC into SiO_2 (dissolved in liquid B_2O_3) + ZrB_2 (unreacted), according to equation (5), with continued oxidation, the second stage of oxidation (point c) involves the oxidation of ZrB_2 into ZrO_2 and B_2O_3 (in solution with SiO_2). One way of preventing the oxidation of ZrB_2 is to dissociate the oxygen environment from the ceramics, if possible, before the second stage of oxidation commences. Alternatively, and more practically, one can take advantage of the kinetic barrier offered to the continuation of oxidation by the liquid B_2O_3–SiO_2 (borosilicate, 70 mol% B_2O_3–30 mol% SiO_2) layer covering the exposed surfaces. The role of borosilicate layer in the oxidation resistance of ZrB_2–SiC ceramics has been reported in many previous studies [5–7,10,11]. Even if B_2O_3 tends to evaporate off, owing to its high vapour pressure (boiling point, 2316 K), the SiO_2-rich layer provides effective oxidation protection [7].

Notably, the preceding discussion is equally valid, if not more, for the oxidation of ZrB_2–SiC ceramics in air ($p_{O_2} = 0.21$ atm), rather than in 1 atm O_2. This is because air is less oxidizing than pure oxygen. To follow the thermodynamic stages of oxidation, a similar isobar of 0.21 atm, which will lie below and parallel to the 1 atm isobar (line *adcdef*) is to be drawn (figure 3).

The 5-atm isobar (line *ghjklm*) presents a different picture. The first stage of oxidation involves the oxidation of ZrB_2 itself along with the formation of liquid borosilicate. Even if liquid borosilicate provides oxidation resistance to the remaining unoxidized ZrB_2, the partial oxidation of the zirconium diboride may spoil its high-temperature properties.

The experimental results of Peng and Speyer [10] support the preceding thermodynamic predictions. Specimens containing ZrB_2 and SiC formed an amorphous, protective borosilicate coating when heated in flowing air at 1733 K. Increasing SiC additions improved the oxidation resistance of the ceramics over an expanding range of temperatures. Guo and Zhang [11] also found that the oxidation of the ceramic ZrB_2–30 vol% SiC was superior to that of the ZrB_2–10 vol% SiC. The oxidation of the ZrB_2–30 vol% SiC followed a cubic kinetics while the ZrB_2–10 vol% SiC followed a

parabolic kinetics. The improved oxidation resistance in the ZrB_2–30 vol% SiC was attributed to the viscosity increase of the glassy (borosilicate) layer.

3.3 *System ZrB_2–B_4C*

The stability diagram of the system ZrB_2–B_4C and the super-imposed 1-atm isobar (*abcdef*), in figure 4, present almost a similar situation to the system ZrB_2–SiC, except for the fact that there is no borosilicate formation. Accordingly, after the first stage of oxidation (point b), during which ZrB_2 is not oxidized, the product is B_2O_3 liquid (pure) plus ZrB_2 (unreacted). In view of the volatility of liquid B_2O_3, it is uncertain how much oxidation resistance this type of ceramics may have. The only recommendation would be to use this ceramics at a lower temperature, perhaps below 1373 K, when the vapour pressure of B_2O_3 is significantly small. In agreement with this, Peng and Speyer [10] reported a poor oxidation resistance of ZrB_2–13.5 vol% B_4C, especially beyond a temperature of 1573 K which marked the onset of accelerated oxidation.

4. Conclusions

The thermodynamics of the oxidation of three-binary ZrB_2-based high temperature ceramics (ZrB_2–TiB_2, ZrB_2–SiC and ZrB_2–B_4C) was studied with the help of four-stability diagrams constructed. It was found that the ZrB_2–TiB_2 ceramics does not have sufficient oxidation resistance in the temperature range of 500–2000 K. ZrB_2 of ZrB_2–SiC ceramics can be protected under 1 atm O_2 or in air if liquid borosilicate (with chosen composition, 70 mol% B_2O_3–30 mol% SiO_2), which is an intermediate product, provides a kinetic barrier to the continuation of oxidation by forming an impervious layer on the exposed surfaces. In contrast, the ZrB_2–B_4C ceramics does not produce the borosilicate because of the absence of SiO_2. In view of the volatility of pure liquid B_2O_3, it is uncertain how much oxidation resistance this type of ceramics may have. The only recommendation would be to use the ZrB_2–B_4C ceramics at lower temperature, perhaps below 1373 K, when the vapour pressure of B_2O_3 is significantly small.

References

[1] Fahrenholtz W G, Hilmas G E, Talmy I G and Zaykoski J A 2007 *J. Am. Ceram. Soc.* **90** 1347
[2] Murata Y and Whitney E B 1969 *Am. Ceram. Soc. Bull.* **48** 698
[3] Murata Y 1973 *Am. Ceram. Soc. Bull.* **52** 255
[4] Zhang X, Hu P, Meng S, Han J and Wang B 2006 *Key Eng. Mater.* **312** 287
[5] Rezaie A, Fahrenholtz W G and Hilmas G E 2006 *J. Am. Ceram. Soc.* **89** 3240
[6] Monteverde F and Bellosi A 2003 *J. Electrochem. Soc.* **150** B552
[7] Rezaie A, Fahrenholtz W G and Hilmas G E 2007 *J. Eur. Ceram. Soc.* **27** 2495
[8] Opila E J and Halbig M C 2001 *Ceram. Eng. Sci. Proc.* **22** 221
[9] Talmy I G, Zaykoski J A, Opeka M M and Dallek S 2001 *Electrochem. Soc. Proc.* **12** 144
[10] Peng F and Speyer R F 2008 *J. Am. Ceram. Soc.* **91** 1489
[11] Guo W M and Zhang G J 2010 *J. Eur. Ceram. Soc.* **30** 2387
[12] Berkowitz-Mattuck J B 1967 *J. Electrochem. Soc.* **114** 1030
[13] Shimada S, Nishisako M, Inagaki M and Yamamoto K 1995 *J. Am. Ceram. Soc.* **78** 41
[14] Singh M and Wiedemeier H 1991 *J. Am. Ceram. Soc.* **74** 724
[15] Harris M, Chaudhary T, Drzal L and Laine R M 1995 *Mater. Sci. Eng. A* **195** 223
[16] Shimada S 1996 *J. Mater. Sci.* **31** 673
[17] Turkdogan E T 1980 *Physical chemistry of high temperature technology* (New York: Academic Press)